Peremennye Zvezdy (*Variable Stars*) **34**, No. 4, 2014

Received December 1; accepted December 10.

Explosion of an LBV star in the galaxy UGC 8246

E.A. Barsukova[1], V.P. Goranskij[2], A.F. Valeev[1,3], and S.S. Kaisin[1]

[1]Special Astrophysical Observatory, Russian Academy of Science, Nizhnij Arkhyz, Karachai-Cherkesia, 369167, Russia; e-mail: bars@sao.ru

[2]Sternberg Astronomical Institute, Lomonosov Moscow University, Universitetski pr., 13, Moscow, 199992, Russia

[3]Kazan Federal University, Kremlevskaya 18, Kazan, 420008, Russia

We present the results of spectroscopy and CCD photometry of the intermediate-luminosity red transient PSN J13100734+3410514 in the galaxy UGC 8246 performed in February and June 2014 with the Russian 6-meter telescope and SCORPIO spectral camera. Our CCD photometry was continued with the Special Astrophysical Observatory's 1-m telescope till November 2014. The star was discovered in late December 2013 at visual brightness $17\overset{\mathrm{m}}{.}6$, which corresponded to the absolute magnitude $M_V = -12\overset{\mathrm{m}}{.}7$, and was identified as a supernova impostor. Spectra taken at the visual brightness level of $19\overset{\mathrm{m}}{.}5$ show composite triple profiles in the H_α and H_β emission lines. We explain the main component of the profiles as radiation from a photoionized extensive gaseous envelope formed by the stellar wind of the progenitor before the outburst. The other two components are treated as radiation from bipolar ejecta. In Balmer line profiles, there is an evidence for a light echo propagating in the surrounding medium after the outburst. Our spectra contain emissions of He I, Na I, Mg I, numerous Fe II emissions, the strongest of which have P Cyg profiles. There are also [O II], [O III], and [S II] emissions of an H II region associated with the transient. The emissions of the region are superimposed on the star spectrum. The light curves show rapid decline and color reddening. Our observations confirm that the UGC 8246 transient was an explosion of a high-mass LBV star.

1 INTRODUCTION

Discoveries of a large number of supernovae using networks of automatic robotic telescopes and preliminary classification of their spectra fill the maximum-luminosity gap between classical novae and supernovae. The optical transients reaching in their outbursts the absolute visual magnitude from -8^{m} to -17^{m} and evolving their spectra to cooler subtypes during outbursts are called Intermediate-Luminosity Red Transients (ILRTs). This family of astrophysical objects is heterogeneous and contains luminous blue variable (LBV) stars with giant eruptions (η Car, low-luminosity SNe 1961V and 1954J with spectra resembling SNe IIn in outbursts), calcium transients like SN 2008S in NGC 6496 or NGC 300 OT having super-AGB stars as progenitors, and luminous red novae like V1006/7 in M31, V838 Mon in the Galaxy, and M85 OT2006–1. Van Dyk et al. (2000) called lower-luminosity SNe IIn "supernova impostors", but later this term was extended to other transients with peak luminosities in the gap (Berger et al. 2009; Smith et al. 2009).

Some LBVs and Galactic red novae turned out to be binaries or multiple systems. The most promising scenario for luminous red novae as merging events in binary systems was suggested by Tylenda & Soker (2006). Tylenda et al. (2011) observed a merging event in the contact binary before the outburst of V1309 Sco as a red nova. On the other hand, Martini et al. (1999) suggested that a red nova phenomenon is due to a nuclear event in a single star, in which a slow shock drives the photosphere outward. Barsukova et al. (2014) specify that this is the phenomenon connected with the adiabatic expansion

of the star envelope after an episodic energy release in the star center. The release may be due to merging of stellar nuclei inside a massive common envelope or to instability of a single stellar nucleus of a young star. η Car, the LBV which experienced a Great Eruption in the mid-1800s accompanied by an episodic mass-loss event, is known as a binary (Corcoran & Ishibashi 2012). The companion is not seen in the spectrum, but it is found to be an O4–O6 giant having mass of 40–50 $M_{\odot}$ based on indirect evidence (Mehner et al., 2010). RXTE X-ray observations show cyclic variability with the 2024-day period that may be the signature of the star's motion in an elliptic orbit with $e = 0.9$ and a semi-major axis $a \approx 15$ AU (Ishibashi et al. 1999). However, the role of this companion in the evolution of η Car and in the Great Eruption scenario is still unknown. Kashi & Soker (2010) and Kashi (2010) suggest that most outbursts of LBV-type systems are powered by gravitational energy released from either a vigorous mass transfer process from the evolved primary star to a main sequence secondary star or a merger of two stars. So, major LBV eruptions can be triggered by stellar companions, and in extreme cases, a short-duration event with a huge mass transfer rate can lead to a bright transient event on time scales of weeks to months. Alternative hypotheses explain LBV eruptions either with enhanced stellar wind episodes when a massive star luminosity sometimes exceeds the Eddington limit, or with interior explosions due to instabilities in stellar nuclei or envelopes that may be pulsational instabilities (Owocki & Shaviv 2012).

Note that one of LBVs in the galaxy NGC 7259, SN 2009ip, previously went through two typical impostor outbursts that reached $M_V = -14^{\rm m}$ in maxima and then became a true core-collapse supernova of –18th absolute magnitude in the peak of brightness (Mauerhan et al. 2013; Margutti et al. 2014).

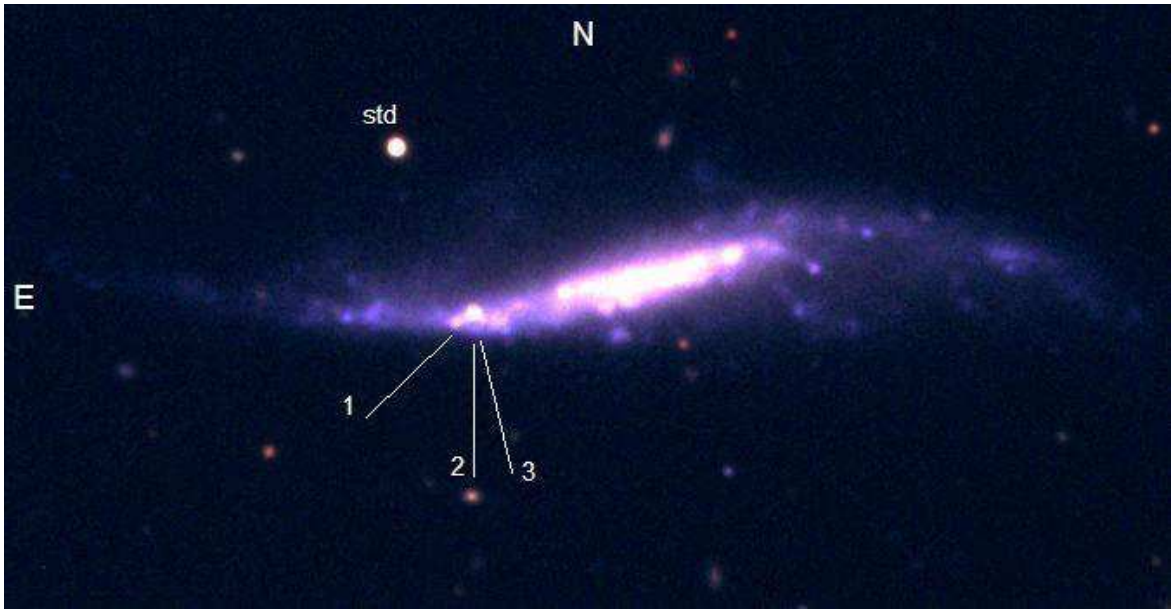

Figure 1.
A color image of the UGC 8246 transient PSN J13100734+3410514 composed from BTA/SCORPIO B, V, and R frames. The image size is $4' \times 2'$. The comparison star is labeled "std". The straight lines marked 1, 2, and 3 are directions of the slit of BTA spectra.

A recent discovery of an LBV-type transient as a possible supernova in UGC 8246 on 2013 December 20.93 UT was reported by Wang and Gao (2013). The object had the R magnitude of approximately 17.75. UGC 8246 is an SB(s)cd type galaxy, its redshift is

$z = 0.002712 \pm 0.000037$ and distance, 11.7 ± 0.8 Mpc; the Galactic interstellar absorption is $A_V = 0\overset{m}{.}03$ (NED). With these parameters, the absolute magnitude of the transient at the time of discovery was $M_V \sim -12\overset{m}{.}7$. Additional photometry acquired in 2013 December was published by Elenin, Wang & Gao, Luppi & Buzzi (CBAT) and by Brimacombe (2014). V-band observations by Wang & Gao, continued during 10 days, show no essential light decay, which strongly suggests that their observations cover the brightness maximum. However, this suggestion may be incorrect in the case of plateau shape of the light curve. Tartaglia et al. (2014a) carried out spectroscopic observations and classified the object as a supernova impostor similar to the prototypical SN 1997bs. SN 1997bs was classified by Van Dyk et al. (2000) as a superoutburst of a very massive luminous blue variable star, analogous to η Car. In the spectrum of the UGC 8246 transient taken on January 8, 2014, Tartaglia et al. (2014a) found H_α emission with an unresolved narrow component superimposed on broader wings (FWHM of about 1800 km s^{-1}). Taking into account scientific interest to SN impostors, we continued spectroscopic and photometric observations of this object.

2 OBSERVATIONS AND DATA REDUCTION

We obtained medium-resolution optical spectra of the transient PSN J13100734+3410514 in UGC 8246 with the SCORPIO focal reducer (Afanasiev & Moiseev 2005) mounted on the 6-m BTA telescope of the Special Astrophysical Observatory (SAO) on 2014 February 8 and June 7. Seeing was measured as FWHM = $2\overset{''}{.}5$ on February 8 and $2\overset{''}{.}3$ on June 7. Additional photometry was performed using the SAO 1-m Zeiss telescope and a CCD photometer with an EEV42-40 chip on 2014 April 3, November 14 and 22. November observations were carried out with the V and R_C filters at good weather conditions with $\sim 1''$ seeing, and the total exposure times were 1200 s or longer.

In the photometric mode with the SCORPIO, we obtained CCD frames with standard B, V and Cousins R filters. The color image generated using these frames is shown in Fig. 1. It demonstrates that the transient occurred in a spiral arm rich in star-forming regions.

To perform relative photometry, we used the comparison star marked "std" in Fig. 1, its SDSS magnitudes being $ugriz$ = 21.03, 18.45, 17.34, 16.91, 16.68. We transferred SDSS magnitudes to BVR_CI_C magnitudes by interpolation using $ugriz$ and UBV AB_{95} magnitudes of α Lyr as described in our previous paper (Barsukova et al. 2012). As a result, the BVR_CI_C magnitudes of the standard star were derived as (18.95, 17.97, 17.25, 16.49). All currently available photometry is presented in Table 1. The light curves plotted using our data and all published observations in the V and R_C filters are shown in Fig. 2.

On February 8, 2014, the spectroscopic camera functioned in the long-slit mode. First it was equipped with the VPHG 1200G grism (nominal spectral range λ $4000 - 5700$ Å, resolution 5 Å, dispersion 0.88 Å pixel^{-1}), and later it was replaced with the VPHG 550G grism (spectral range λ $3500 - 7200$ Å, resolution 10 Å, dispersion 2.1 Å pixel^{-1}). Actual resolution measured using emission lines of night sky was 5.4 Å for the VPHG 1200G grism and 14.6 Å for VPHG 550G. In the first spectrum, we found an essential contribution of a nearby galactic H II region in the brightest lines of the stellar spectrum, so we took spectra with different position angles of the slit. Slit locations at different telescope pointings are shown as straight lines in Fig. 1 and they are listed in Table 2 for individual spectra. On June 7, 2014, we used only the VPHG 550G grism. Spectra were reduced using standard ESO MIDAS procedures for the long-slit mode. Basic parameters

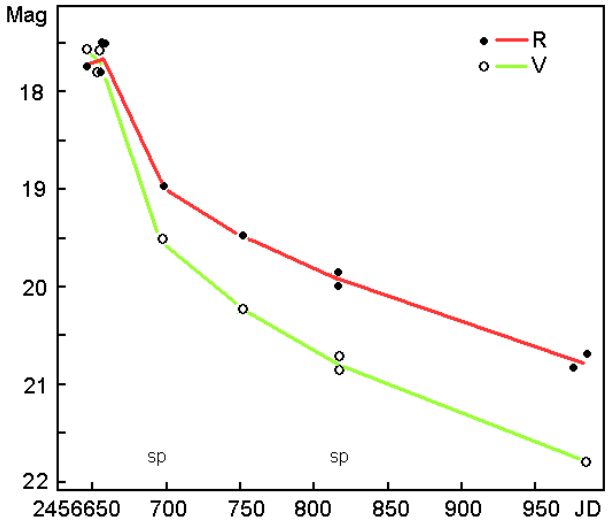

Figure 2.
V and R_C light curves of the transient PSN J13100734+3410514 in UGC 8246. Dates of BTA/SCORPIO spectroscopy are marked "sp".

of our spectra are collected in Table 2. The blue and green spectral regions are displayed in Fig. 3, and the whole optical spectra are presented in Fig. 4. The wavelengths in these figures have been corrected with respect to bright emission components of Balmer lines.

3 RESULTS

Analyzing published early non-homogeneous observations presented in Table 1, one can suggest that the star had a $V - R_C$ color index about zero at the outburst maximum. We do not know the interstellar reddening in the galaxy UGC 8246 and therefore can determine only the upper limit to the bolometric magnitude ($M_{bol} \leq -13\overset{\mathrm{m}}{.}0$) and the lower limit to the effective temperature ($\log T_e \geq 4.48$). Our February photometry taken 50 days after the maximum gave the following magnitudes and color indices: $V = 19\overset{\mathrm{m}}{.}51$, $B - V = 0\overset{\mathrm{m}}{.}71$, $V - R_C = 0\overset{\mathrm{m}}{.}54$. Reddening continued in June; on the 169th day after the light maximum, $V - R_C$ was $0\overset{\mathrm{m}}{.}86$. In November, on the 336th day at the level of $V = 21\overset{\mathrm{m}}{.}8$, the star became even redder, with $V - R_C = 1\overset{\mathrm{m}}{.}09$. The star had a primary decay of $2\overset{\mathrm{m}}{.}0$ V in 50 days and a nonlinear secondary decay both in the V and R_C bands. By the 169th day after maximum, the speed of the decay decreased to about $0\overset{\mathrm{m}}{.}7$ V in 100 days.

The spectrum of the UGC 8246 transient taken in February was rich in emission lines. It resembled spectra of Fe II-class novae in the fireball stage (e.g., see Williams 2012; we used the finding list of optical emission lines in his Table 2 for identification). The lines we have identified are listed in Table 3. The strongest emission lines in our spectra are Balmer lines, [O II], and [O III]. Oxygen lines are evidently radiated in the nearby H II regions in the spiral arm of the galaxy. As seen in Fig. 5, the regions of [O III] emission are superimposed on the stellar spectrum only partly. Otherwise, this figure shows that the main component of H_β emission mostly has a stellar origin. But oxygen lines are located at the same radial velocity, +920 km s^{-1}, as the strongest H_β component. Direct images taken in the R_C filter in November confirm the association of the transient with a compact H II region, the brightest part of which is located in $1\overset{''}{.}0$ east and $0\overset{''}{.}5$ south of

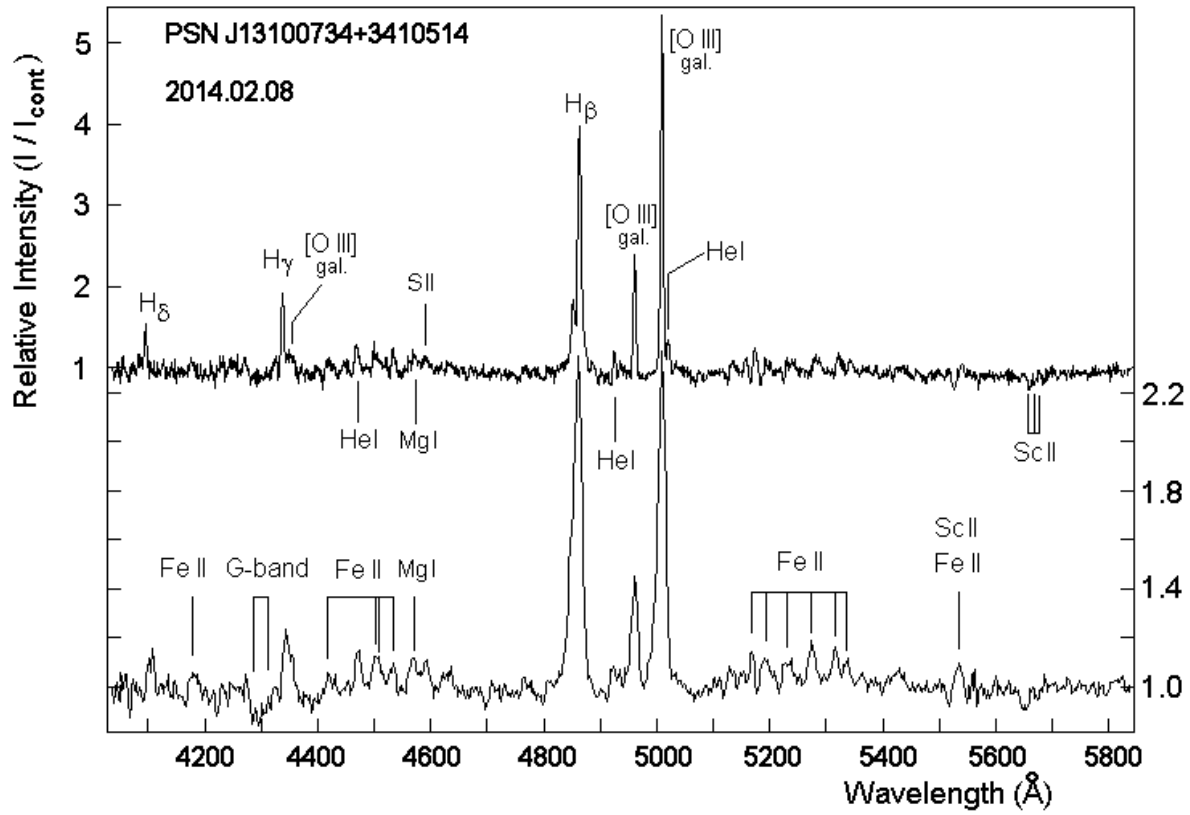

Figure 3.
BTA/SCORPIO spectra of the UGC 8246 transient in the blue and green regions on February 8, 2014. Both spectra are corrected for the redshift and presented for zero velocity. Top: the higher resolution spectrum; bottom: the same fragment of the lower resolution spectrum.

the transient. These spectra and the direct images definitely provide evidence that the explosion of this transient has happened in the active star forming region rich in young massive stars.

The equivalent widths of Balmer lines on February 8 were the following: EW(H_α) = −180 Å; EW(H_β) = −37 Å; EW(H_γ) = −11 Å; EW(H_δ) = −3 Å. H_ε, in a blend with Ca II H, form a deep absorption line. On June 7, the equivalent widths changed to –350 Å (H_α), –41 Å (H_β), and –7 Å (H_γ).

With the best resolution of 5.4 Å, the H_β line profile looks complex (Fig. 6). The strongest narrow component has FWHM = 320 ± 30 km s^{-1} after correction for the spectral resolution. The profile extends over FWZI = 2200 km s^{-1}. Additionally, there is another weak blue narrow emission component in the profile, displaced by −660 km s^{-1} with respect to the main component and having approximately the same half width, 320 km s^{-1}. A dip between these components is at the velocity of –380 km s^{-1} and looks like an absorption. Such profiles with an absorption component are rare in spectra of SN impostors but do exist. With wings, an absorption dip and a narrow component, the H_β line profile of UGC 8246 transient resembles Balmer line profiles of the type IIP supernova 1994W in NGC 4041 (Sollerman et al. 1998), but that was a true and extremely luminous supernova. A similar shape of Balmer line profiles was observed by Humphreys et al. (2012) in the spectrum of the peculiar type IIn SN or impostor 2011ht in UGC 5460. That star had reached $M_V = -17^m$ in maximum. However, the wing span in the profiles of these two supernovae was 4 times larger than that of the

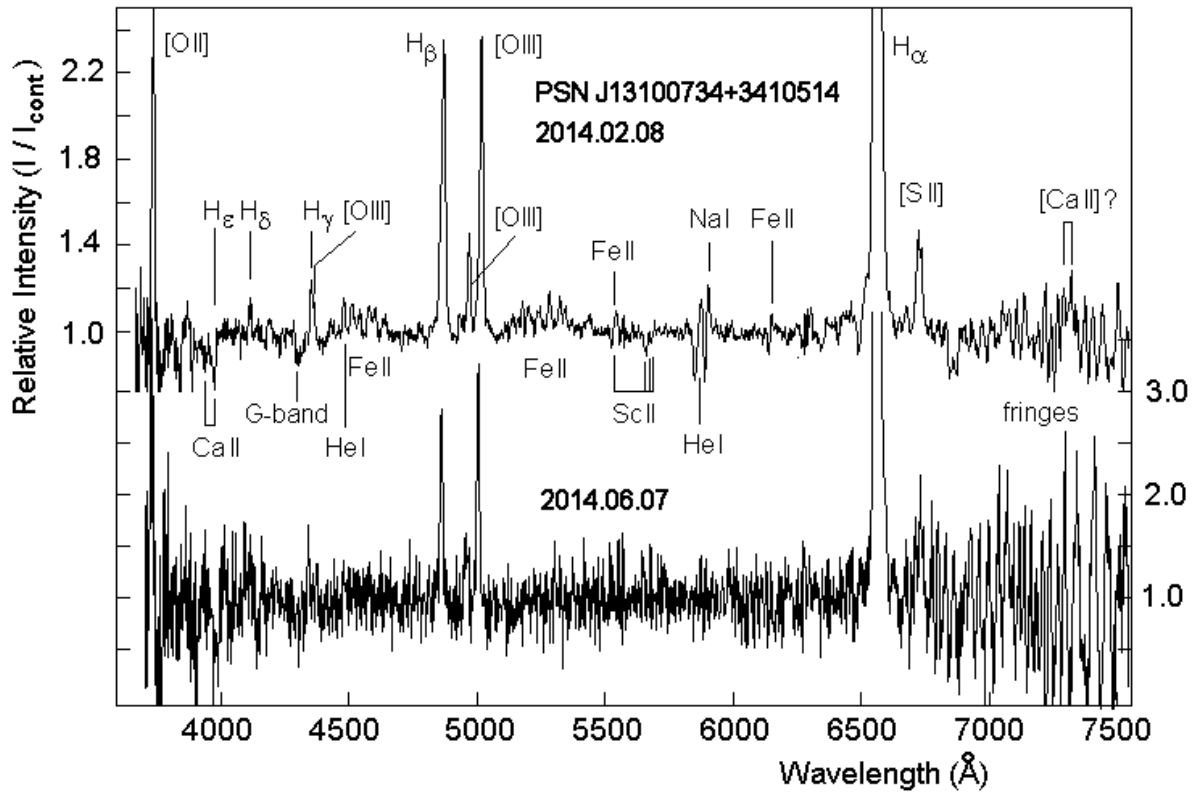

Figure 4.
A comparison of lower resolution spectra of the UGC 8246 transient taken with BTA/SCORPIO on February 8 and June 7, 2014. Both spectra are corrected for the redshift.

UGC 8246 transient. Also, wings of the H_β line profile are twice narrower than wings of the same profile of the "calcium transient" in NGC 5775 observed by us (Barsukova et al. 2012). There was no absorption component in the profile of that transient. The narrow component in H_α profile of the UGC 8246 transient was poorly resolved with the VPHG 550G grism. The line displayed a blue shoulder that confirmed the presence of a similar blue narrow component at the velocity about –660 km s^{-1}. Explaining profiles of similar shape in Balmer lines of SN 1994W, Chugai et al. (2004) identified their components with a photoionized expanding circumstellar envelope, shocked cool gas in the forward post-shocked region, and multiple Thompson scattering in the envelope. Probably cool gas is responsible for the absorption component in the profiles of Balmer lines. The models gave a rather deep absorption component in a case of homologous expansion of the ejecta without post-explosion radiative acceleration but did not take into consideration light echo in the circumstellar medium.

One can expect that the light echo of an LBV explosion expanding through the circumstellar envelope formed by stellar wind of the progenitor should influence the Balmer line profiles. An external observer can see only those illuminated dust particles or emissive excited atoms that are located on the surface of the ellipsoid with the flare source in one focus, and the observer in the other one. In this case, the total light path from the source to a particle and of the reflected light from the particle to the observer is the same for all visible particles at the time t after the flare, namely $c \cdot t$. During the first weeks after the outburst, the ellipsoid is narrow and elongated along the line of sight. Then the photoionization front in the expanding gaseous envelope visible for the observer

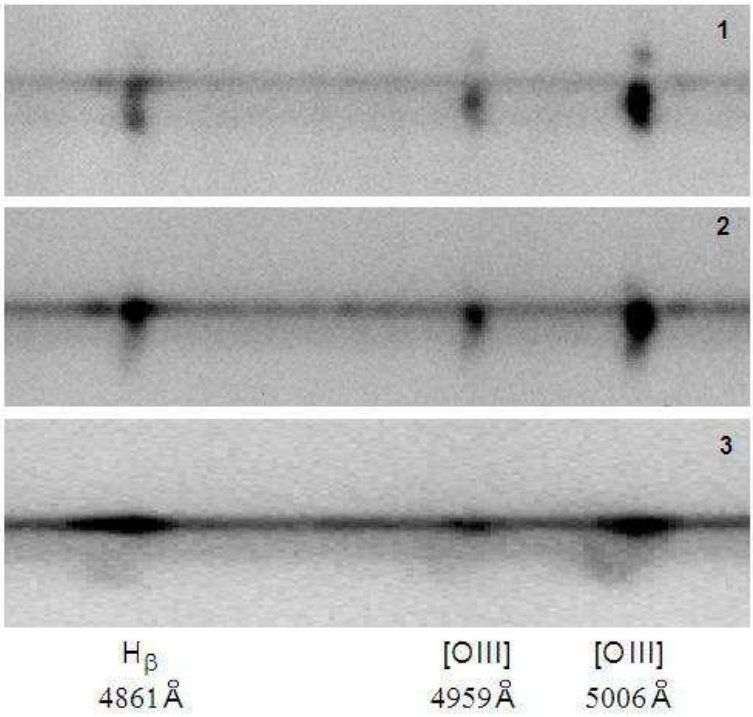

Figure 5.
Two-dimensional BTA/SCORPIO spectrograms of the UGC 8246 transient in the λ 4800 − 5100 Å wavelength range for the three slit locations. The numbers correspond to slit locations displayed in Fig. 1. [O III] emissions evidently belong to a close star-forming H II region, and the transient is located at its edge. At the same time, the photos show that the radiation of the blue component belongs just to the star, but the main component is contaminated by radiation of the star-forming region which has the same radial velocity as the star.

in the first weeks includes only the part of the envelope that is located along the line of sight and moving to the observer. The light from the excited gas at the opposite side of the envelope and from other parts of it has not yet reached the observer. Thus, in the first weeks, we expect to have more negative velocity of the main emission component relative to its velocity during the last stages. To test the assumption on the light echo, we measured velocities of peaks in the H_α and H_β profiles in the spectrum by Tartaglia et al. (2014a) taken on January 8, 2014 and found 820 and 850 km s^{-1}, respectively, against 970 and 920 km s^{-1} in our February 8 spectra. So the velocity difference is really present, and is equal to -110 ± 40 km s^{-1}. Later, the visible front of ionization will get to the opposite side of the wind envelope, with velocities directed away from the observer, and the central-peak velocity will increase. Our spectrum taken on June 7 gives larger velocities, 1060 km s^{-1} for H_α and 960 km s^{-1} for H_β (these values were corrected with respect to galactic [O III] lines). Note that the presence of a negative excess in the velocity of the main emission component of H_α on January 8, 2014 confirms the hypothesis that the transient was discovered at an early stage of the outburst and testifies against a plateau stage. Thus, the effects of light echo in Balmer-line profiles in the spectra of SN impostors are strong and should be taken into account in the spectral line modeling.

We have tried to separate components of the H_β line profile (Fig. 6) using the MIDAS procedure DEBLEND/LINE. These components were fitted with Gaussian functions. The fit with a broad component along with two narrow ones represents the total profile badly, especially to the red side. The observed curve runs evidently above the model one. An

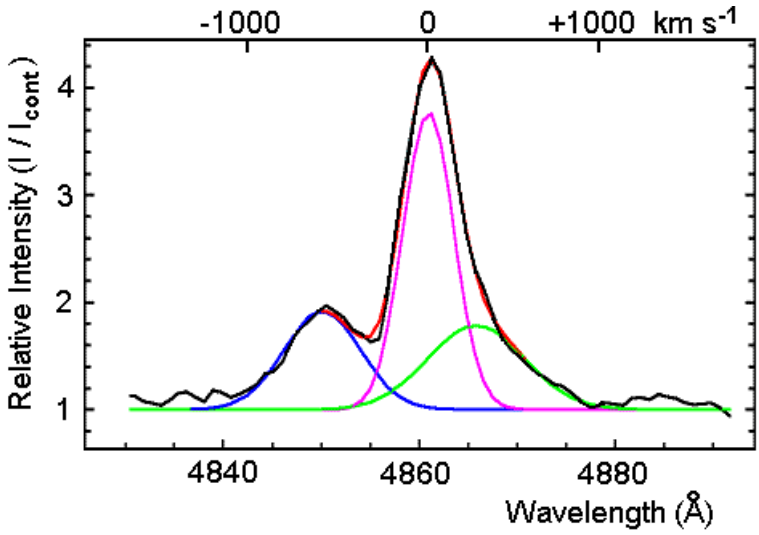

Figure 6.
The H_β line profile in the spectrum with the resolution of 5.4 Å taken on 2014 February 8 (black curve). Gaussian components are shown in blue, pink, and green colors. The model profile defined as the sum of the three components is plotted as the red curve.

attempt to fit the profile including one absorption component represents the data better but results in a very broad main component and a broad absorption which eats up half of main emission width. Such a model is hard to explain physically. But the fit without any broad component and with three narrow ones is the best. In short, the red excess in the profile can be successfully fitted with an additional Gaussian. Parameters of the components in this model are the following: for the blue one, $v_R = -670 \pm 15$ km s^{-1}, FWHM $= 570 \pm 40$ km s^{-1}, EW $= -8.9$ Å; for the central one, $v_R = 0 \pm 20$ km s^{-1} (adopted), FWHM $= 376 \pm 15$ km s^{-1}, EW $= -18.0$ Å; for the red one, $v_R = +300 \pm 70$ km s^{-1}, FWHM $= 715 \pm 85$ km s^{-1}, EW $= -9.7$ Å. Note that the FWHM values in this model include the instrumental profile. The fitting and its three Gaussian components are shown in Fig. 6.

We have an alternative explanation of the H_β line profile based on this fitting. A separate narrow blue component may be the radiation of a frontal lobe of bipolar ejecta thrown out in the direction of the observer, while the opposite receding lobe is partly covered by the volume of the approaching lobe. The non-covered radiation of the receding lobe is visible in the red part of the profile. Note that a contribution from the H II region may be partly added to the red component (see Fig. 5). Such a bipolar eruption formed the "Homunculus Nebula" of η Car in the mid-1800s explosion. The lobes in the Homunculus are known to be expanding radially with velocities in the range of 650–700 km s^{-1} (Davidson & Humphreys 1997) which is in agreement with 670 km s^{-1} for the UGC 8246 transient. However, the UGC 8246 transient outburst was not so long in duration, only 200 days vs. 20 years for η Car. In this case, the dip between two narrow components in the profile of H_β cannot be treated as an absorption.

The rich weak-line spectrum indicates a dense environment containing evolved material ejected from the progenitor by the stellar wind in the super-Eddington regime. There are many Fe II emission lines in the spectrum, the strongest ones have P Cyg profiles. The absorption component of the strongest Fe II 5169 Å line is located at the velocity of -400 km s^{-1}. Forbidden emissions are absent in the stellar spectrum, but they are present in the spectrum of the galaxy environment. The stellar spectrum indicates low

excitation and absence of a hot ionizing source. He I 5876 Å is very strong, it has a P Cyg profile; its absorption component is centered at the velocity of –1500 km s^{-1} and expands to –1850 km s^{-1} with respect to the center of the emission component. The center of the emission component is displaced by –400 km s^{-1} against main components of the Balmer lines. The profile looks strange and unlike any other lines, and there is an assumption that it is being formed entirely in the ejecta, not in the wind. He I 4471 Å is also strong, so we have to identify emission lines at 4922 and 5016 Å as He I lines, though they can contain some contribution from close Fe II components. The Na I D_2D_1 blend has a P Cyg profile and is as strong as He I 5876 Å. The absorption component of Na I is displaced to the blue side from the emission component's center by 700 km s^{-1}.

The Ca II H & K lines are in absorption. In the spectra, we also identify the Mg I 4571 Å intercombination line that may be formed in massive and rarefied nebulae, and sometimes occurs in ejecta of red novae (Goranskij & Barsukova 2007). Recently Tartaglia et al. (2014b) found absorption lines of Ba II and Sc II in the spectra of the SN impostor 2007sv that exploded in the galaxy UGC 5929; these species are not met in the spectra of classical novae. The presence of Sc II, Mg II, and Si II was noted in the spectra of SN 1994W (Chugai et al. 2004). We tried to find these lines in our spectra of the UGC 8246 transient, and the attempt seems to be successful only for Sc II. There is an obvious depression at λ5640–5684 Å that cannot be explained by absorption of other chemical elements except Sc II. The line of Sc II 5526 Å can contribute to the absorption component of the Fe II 5535 Å P Cyg-type profile. We also identified a strong absorption feature located towards short wavelengths from H_γ at λ4294–4315 Å, like the G band in early G-type stars. This molecular CH band was found in the spectrum of the η Car-type transient SN 2011ht by Humphreys et al. (2012).

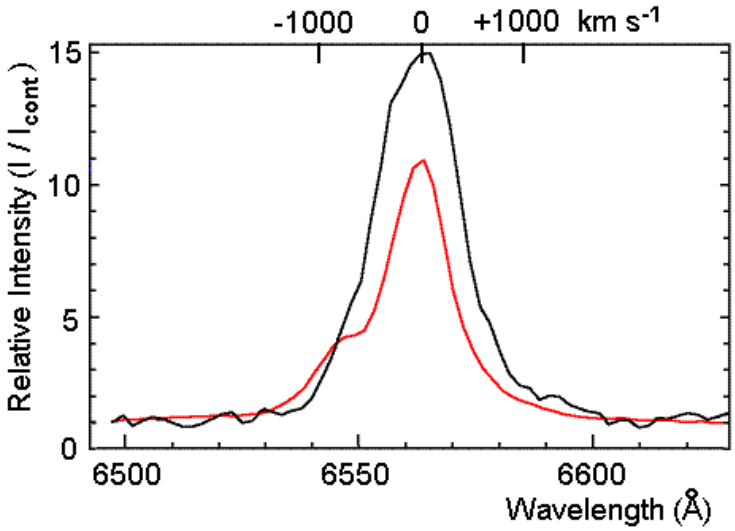

Figure 7.
Evolution of the H_α line profile for 119 days between 2014 February 8 (red curve) and 2014 June 7 (black curve) in the BTA/SCORPIO normalized spectra with the resolution of 14.6 Å.

In the low-resolution noisy spectrum taken on June 7 (on the 169th day after maximum), when the object's brightness was at the level of $20^m.8$ in the V band, only the strongest lines of the transient and the galaxy are visible. The Balmer lines definitely belong to the transient: the star's continuum can be distinguished in the spectrum, and the stellar image is visible in the direct frames. Figure 7 compares the H_α line profiles in the

February 8 and June 7 spectra. The narrow H_α line became noticeably broader on June 7 than on February 8. In spite of low resolution, the red and blue components stay visible in the profile as shoulders. Note that these components may be the radiation of bipolar ejecta. The half width of the profile increased from 300 to 700 km s^{-1}. These estimates were corrected for the spectral resolution, and their accuracy is about 50 km s^{-1}. Both profiles are plotted in intensity units relative to the stellar continuum. The star faded between these dates by $1\overset{m}{.}0$ in the R_C band. The contribution of continuum in the R_C band changed between these dates from 82 to 78 per cent. As the H_α flux declined slower than the continuum, the equivalent width of the H_α line increased its absolute value from 180 to 350 Å. We explain the broadening of the H_α line by two reasons. First, it is the radiative acceleration of the stellar wind. The second reason is the expansion of visible volume of the photoionized region of stellar wind due to expanding light echo.

The observations of LBV-type transient remnants with the *Hubble* space telescope or *Spitzer* infrared space telescope show that the LBV stars survive in their explosions. Some of them undergo repeated explosions. Thus, future observations of the UGC 8246 transient are encouraged.

4 CONCLUSIONS

We present the results of our spectroscopy and CCD photometry of the intermediate-luminosity red transient PSN J13100734+3410514 in UGC 8246 performed in February and June, 2014 with the Russian 6-m BTA telescope and SCORPIO spectral camera and follow-up CCD photometry with the SAO 1-m telescope.

The transient showed a number of characteristics typical of LBV stars with giant eruptions. Namely, the amplitude of the outburst exceeded three magnitudes; the bolometric magnitude at maximum was evidently above the Humphreys–Davidson limit (the upper boundary of the supergiant luminosities in the $M_{bol} - T_{eff}$ diagram; see Humphreys & Davidson 1979); a significant reddening of the spectrum occurred during the outburst decline; the spectrum is typical of LBV stars; moderate wind velocities are characteristic of LBV stars; a possible bipolar ejecta signature was seen in the Balmer line profiles. There is an evidence for a light echo of the outburst expanding in the surrounding gaseous medium after the outburst. We assume, like other researchers, that this transient was an explosion of a high-mass LBV star.

Acknowledgments.

This work was supported by the Russian Foundation for Basic Research (RFBR) with the grants 13-02-00885 and 14-02-00759. E.A.B. thanks the President of the Russian Federation for the grant supporting the Leading scientific school NSh-4308.2012.2. A.F.V. thanks the President for grants for young PhD researchers MK-6686.2013.2 and MK-1699.2014.2 and the RFBR for the grant 12-02-31548. We thank Drs. D.Yu Tsvetkov and O.V. Maryeva for discussion. Observations with the Russian 6-m telescope are financially supported by the Ministry of Education and Science of Russian Federation (agreement No. 14.619.21.004, project identifier RFMEFI61914X0004). This research has made use of the Sloan Digital Sky Survey and of the NASA/IPAC Extragalactic Database (NED).

References:

Afanasiev, V.L., Moiseev, A.V., 2005, *Astronomy Letters*, **31**, 194

Brimacombe, J., 2014,
http://spacefinalfrontier.blogspot.ru/2014/02/luminous-blue-variable-psn.html

Barsukova, E.A., Fabrika, S.N., Goranskij, V.P., Valeev, A.F., 2012, *Variable Stars*, **32**, No. 2
Barsukova, E.A., Goranskij, V.P., Valeev, A.F., Zharova, A.V., 2014, *Astrophys. Bull.*, **69**, 67
Berger, E., Soderberg, A.M., Chevalier, R.A. et al., 2009, *Astrophys. J.*, **699**, 1850
Chugai, N.N., Blinnikov, S.I., Cumming, R.J., et al., 2004, *MNRAS*, **352**, 1213
Corcoran, M.F., Ishibashi, K., 2012, in *Eta Carinae and the Supernova Impostors*, R. Davidson & R.M. Humphreys (eds.), Springer, New York, p.195
Davidson, K., Humphreys, R.M., 1997, *Ann. Rev. Astron. & Astrophys.*, **35**, 1
Goranskij, V.P., Barsukova, E.A., 2007, *Astron. Reports*, **51**, 126
Humphreys, R.M., Davidson, K., 1979, *Astrophys. J.*, **232**, 409
Humphreys, R.M., Davidson, K., Jones, T.J., et al., 2012, *Astrophys. J.*, **760**, 93
Ishibashi, K., Corcoran, M.F., Davidson, K., et al., 1999, *Astrophys. J.*, **524**, 983
Kashi, A., Soker, N., 2010, *arXiv*:1011.1222
Kashi, A., 2010, *AIP Conference Proc.*, **1314**, 55
Margutti, R., Milisavljevic, D., Soderberg, A.M. et al., 2014, *Astrophys. J.*, **780**, 21
Martini, P., Wagner, R.M., Tomaney, A. et al., 1999, *Astron. J.*, **118**, 1034
Mauerhan, J.C., Smith, N., Filippenko, A.V. et al., 2013, *MNRAS*, **430**, 1801
Mehner, A., Davidson, K., Ferland, G.J. et al., 2010, *Astrophys. J.*, **710**, 729
Owocki, S.P., Shaviv, N.J. 2012, in *Eta Carinae and the Supernova Impostors*, K. Davidson & R.M. Humphreys (eds.), Springer, New York, p.275
Smith, N., Ganeshalingam, M., Chornock, R. et al., 2009, *Astrophys. J.*, **697**, L49
Sollerman, J., Cumming, R.J., Lundquist, P., 1998, *Astrophys. J.*, **493**, 933
Tartaglia, L., Pastorello, A., Benetti, S. et al., 2014a, *Astronomer's Telegram*, No. 5737
Tartaglia, L., Pastorello, A., Taubenberger, S. et al., 2014b, *arXiv*:1406.2120
Tylenda, R., Soker, N. 2006, *Astron. & Astrophys.*, **451**, 223
Tylenda, R., Hajduk, M., Kaminski, T. et al., 2011, *Astron. & Astrophys.*, **528**, 114
Van Dyk, S.D., Schuyler, D., Peng, C.Y. et al, 2000, *Publ. Astron. Soc. Pacific*, **112**, 1532
Wang, B., Gao, X., 2013, CBAT (http://www.cbat.eps.harvard.edu/unconf/followups/J13100734+3410514.html)
Williams, R., 2012, *Astron. J.*, **144**, 98

Table 1: Available photometry of PSN J13100734+3410514

Date	JD hel. 2400000+	mag	Filter	Source
2013.12.20	56647	17.75	R	Bin Wang, Xing Gao (CBAT)
2013.12.20	56647	17.6	V	Bin Wang, Xing Gao (CBAT)
2013.12.28	56655	17.8	R	L. Elenin (CBAT)
2013.12.28	56655	17.8	V	Bin Wang, Xing Gao (CBAT)
2013.12.29	56656	17.6	V	Bin Wang, Xing Gao (CBAT)
2013.12.30	56657	17.5	R	F. Luppi, L. Bussi (CBAT)
2013.12.31	56658	17.51	V	Brimacombe (2013) $\pm$0.12
2014.02.08	56697.5559	19.51	V	BTA/SCORPIO
2014.02.08	56697.5574	20.22	B	BTA/SCORPIO
2014.02.08	56697.5589	18.97	R_C	BTA/SCORPIO
2014.04.03	56751.3947	20.23	V	Zeiss-1000/EEV42-40
2014.04.03	56751.4096	19.67	R_C	Zeiss-1000/EEV42-40
2014.04.03	56751.4138	20.51	B	Zeiss-1000/EEV42-40
2014.06.07	56816.2918	19.85	R_C	BTA/SCORPIO
2014.06.07	56816.2945	20.71	V	BTA/SCORPIO
2014.06.07	56816.2965	20.85	V	BTA/SCORPIO
2014.06.07	56816.2984	19.99	R_C	BTA/SCORPIO
2014.11.14	56975.6144	20.81	R_C	Zeiss-1000/EEV42-40
2014.11.22	56983.5790	21.83	V	Zeiss-1000/EEV42-40
2014.11.22	56983.5963	20.67	R_C	Zeiss-1000/EEV42-40

Table 2: Spectra of PSN J13100734+3410514 taken with BTA/SCORPIO*)

Time of mid-exposure, UT	Exposure, s	λ Å	S/N,	Grism	Resolution, Å	Slit location
2014 Feb 08.984	1200	4053–5848	7	VPHG1200G	5.4	1
2014 Feb 09.027	2400	4053–5848	15	VPHG1200G	5.4	2
2014 Feb 09.106	2400	3644–7906	25	VPHG550G	14.6	3
2014 Jun 06.970	600	3716–7905	2	VPHG550G	14.6	3

*) Original normalized spectra in ASCII code are available in the Internet at http://jet.sao.ru/∼bars/spectra/psn1310/

Table 3: Line identifications

Element	λ_0, Å	Notes
[O II]	3727	blend, galaxy
Ca II	3934	absorption
Ca II	3968	blend with H_ϵ
H_ϵ	3970	absorption
H_δ	4102	P Cyg
Fe II	4179	
G band	4294–4315	CH molecular absorption
H_γ	4340	P Cyg
[O III]	4363	galaxy
Fe II	4417	
He I	4471	
Fe II	4508	
Fe II	4515	
Fe II	4534	
Mg I]	4571	intercombination line
S II?	4591	blend
H_β	4861	P Cyg
He I	4922	P Cyg
[O III]	4959	galaxy
[O III]	5007	galaxy
He I	5016	
Fe II	5169	P Cyg
Fe II	5198	
Fe II	5235	
Fe II	5276,5284	blend
Fe II	5317	P Cyg
Fe II	5333,5337	blend
Fe II	5535	
Sc II	5526	
Sc II	5667	blend, absorption
He I	5876	P Cyg
Na I D_2,D_1	5889,5892	P Cyg
Fe II	6148	P Cyg
H_α	6563	emission
[S II]	6716,6731	galaxy
[Ca II]?	7296,7329	weak, blend?